Probing the Ligand-binding Domain of the mGluR4 Subtype of Metabotropic Glutamate Receptor*

(Received for publication, April 30, 1999, and in revised form, August 9, 1999)

David R. Hampson‡§, Xi-Ping Huang‡, Roman Pekhletski‡, Vanya Peltekova‡, Geoffrey Hornby‡, Christian Thomsen¶, and Henning Thøgersen‖

From the ‡Faculty of Pharmacy and the Department of Pharmacology, University of Toronto, Toronto, Ontario M5S 2S2, Canada and the Departments of ¶Molecular Pharmacology and ‖Medicinal Chemistry, Novo Nordisk A/S, 2760 Måløv, Denmark

Metabotropic glutamate receptors (mGluRs) are G-protein-coupled glutamate receptors that subserve a number of diverse functions in the central nervous system. The large extracellular amino-terminal domains (ATDs) of mGluRs are homologous to the periplasmic binding proteins in bacteria. In this study, a region in the ATD of the mGluR4 subtype of mGluR postulated to contain the ligand-binding pocket was explored by site-directed mutagenesis using a molecular model of the tertiary structure of the ATD as a guiding tool. Although the conversion of Arg^{78}, Ser^{159}, or Thr^{182} to Ala did not affect the level of protein expression or cell-surface expression, all three mutations severely impaired the ability of the receptor to bind the agonist L-[^{3}H]amino-4-phosphonobutyric acid. Mutation of other residues within or in close proximity to the proposed binding pocket produced either no effect (Ser^{157} and Ser^{160}) or a relatively modest effect (Ser^{181}) on ligand affinity compared with the Arg^{78}, Ser^{159}, and Thr^{182} mutations. Based on these experimental findings, together with information obtained from the model in which the glutamate analog L-serine *O*-phosphate (L-SOP) was "docked" into the binding pocket, we suggest that the hydroxyl groups on the side chains of Ser^{159} and Thr^{182} of mGluR4 form hydrogen bonds with the α-carboxyl and α-amino groups on L-SOP, respectively, whereas Arg^{78} forms an electrostatic interaction with the acidic side chains of L-SOP or glutamate. The conservation of Arg^{78}, Ser^{159}, and Thr^{182} in all members of the mGluR family indicates that these amino acids may be fundamental recognition motifs for the binding of agonists to this class of receptors.

Metabotropic glutamate receptors (mGluRs)[1] are a family of eight G-protein-coupled receptors that are expressed throughout the central nervous system and in sensory cells of the retina and tongue. The mGluR family has been divided into three subgroups based on sequence homology, pharmacology, and signal transduction properties; in cell lines, group I mGluRs couple to phosphoinositide turnover, whereas group II and III receptors couple to the inhibition of forskolin-stimulated cAMP via G_i/G_o proteins (1, 2). mGluR4 together with mGluR6, mGluR7, and mGluR8 constitute the group III subclass of mGluRs that are selectively sensitive to the phosphono derivative of L-glutamate, L-amino-4-phosphonobutyric acid (L-AP4), and the endogenous amino acid L-serine *O*-phosphate (L-SOP).

The group III mGluRs are important regulators of synaptic transmission in the central nervous system. Electrophysiological experiments have shown that activation of L-AP4-sensitive receptors causes a suppression of synaptic transmission by inhibiting neurotransmitter release from nerve terminals (3), and immunocytochemical studies have confirmed that group III mGluRs are localized presynaptically (4–6). The characterization of mutant mice lacking the mGluR4 subtype of mGluR has provided additional insight into the function of this receptor in the nervous system. For example, observations from electrophysiological analyses demonstrating impaired presynaptic functions in the mutant mice led to the suggestion that this receptor may be required for sustaining synaptic transmission during periods of high-frequency neurotransmission (7). Behavioral studies on mGluR4 mutant mice have shown that this receptor plays a role in motor and spatial learning (7, 8). The potential use of group III mGluR ligands as therapeutic agents in epilepsy and neurodegenerative disorders has provided a persuasive argument for conducting more detailed structural analyses of this class of neurotransmitter receptors (9, 10).

The amino acid sequences of the mGluRs are homologous to the periplasmic amino acid-binding proteins in bacteria (11), the calcium-sensing receptor of the parathyroid gland (12, 13), the $GABA_B$ receptors (14–16), a group of mammalian pheromone receptors (17), and a class of taste receptors expressed in lingual tissue (18). The basic structural domains of mGluRs include a large extracellular amino-terminal domain (ATD), seven putative transmembrane domains, and an intracellular carboxyl terminus. The homology of the ATDs of mGluRs to the leucine/isoleucine/valine-binding protein (LIVBP) and other bacterial periplasmic binding proteins that mediate the transport of amino acids in prokaryotes is fortuitous because the mGluRs appear to possess a similar three-dimensional fold and the crystal structures of the bacterial proteins are known (11).

Data obtained from experiments on chimeric constructs of the ATD of human mGluR4 with the transmembrane domains and carboxyl-terminal regions of mGluR1b (19) and constructs containing various segments of the ATD of rat mGluR2 and the

* This work was supported by grants from the Medical Research Council of Canada and by the European Commission. The costs of publication of this article were defrayed in part by the payment of page charges. This article must therefore be hereby marked "*advertisement*" in accordance with 18 U.S.C. Section 1734 solely to indicate this fact.

§ To whom correspondence should be addressed: Faculty of Pharmacy, University of Toronto, 19 Russell St., Toronto, Ontario M5S 2S2, Canada. Tel.: 416-978-4494; Fax: 416-978-8511; E-mail: d.hampson@utoronto.ca.

[1] The abbreviations used are: mGluRs, metabotropic glutamate receptors; L-AP4, L-amino-4-phosphonobutyric acid; L-SOP, serine *O*-phosphate; $GABA_B$, γ-aminobutyric acid, type B; ATD, amino-terminal domain; LIVBP, leucine/isoleucine/valine-binding protein; HEK, human embryonic kidney; PCR, polymerase chain reaction; L-CCG-1, (2*S*,3*S*,4*S*)-CCG/(2*S*,1′*S*,2′*S*)-2-(carboxycyclopropyl)glycine; CPPG, (*RS*)-α-cyclopropyl-4-phosphonophenylglycine; PBS, phosphate-buffered saline.

transmembrane domain and carboxyl terminus of mGluR1a (20) indicated that pharmacological selectivity is conferred by residues located in the ATDs of mGluRs. More recent studies demonstrating that the ATDs of mGluR1 (21) and mGluR4 (22) can be expressed as soluble proteins that are secreted from transfected cells and that retain ligand-binding capabilities have corroborated the concept that the primary determinants of ligand binding to mGluRs are contained within the ATDs. In this study, we have employed molecular modeling in conjunction with site-directed mutagenesis to probe the ligand-binding pocket of mGluR4. Our results indicate that three conserved amino acids present in the ATDs may be key determinants of ligand binding to all members of the mGluR family.

EXPERIMENTAL PROCEDURES

Molecular Modeling—The three-dimensional structure of the proposed ligand-binding domain of rat mGluR4 was formulated by homology modeling using the experimentally determined structure of the closed form of LIVBP from *Escherichia coli* and the strategy outlined by Blundell *et al.* (23). The atomic coordinates for the closed form of LIVBP with leucine in the binding pocket were kindly provided by Dr. F. A. Quiocho (Baylor College of Medicine). The QUANTA program (Version 97, MSI Corp.) and the SYBYL program (Version 6.4, Tripos Associates) were used to view the model that encompassed the region from Gly^{47} to Lys^{490} in the ATD of mGluR4. The sequence alignment used in the mGluR4 model has been described previously (11). Backbone atom coordinates were assigned the corresponding residue coordinates from the crystal structure of LIVBP, and side chain atom coordinates were based on maximal side chain atom fitting to the LIVBP structure. Regions with insertions or deletions were modeled using known substructures identified by loop-searching techniques; regions 1–46, 125–149, 353–401, and 426–439, which are absent in LIVBP, were not included in the model. The L-SOP molecule was docked into the binding site of mGluR4 in an orientation that corresponds to that observed for leucine binding to LIVBP. The model was energy-optimized using a restrained energy minimization with additional constraints applied to the backbone regions based on the x-ray structure of LIVBP using the CHARMm force field. A steepest descent followed by a conjugate gradient method were used for energy minimization until the energy change per cycle was <0.0001 kcal/mol.

Expression Vectors, Mutagenesis, and Transfections—For the expression of wild-type mGluR4a in human embryonic kidney cells (HEK-293-TSA-201), the *Bgl*II-*Eco*RI fragment of mGluR4a in the pBluescript SK^- phagemid (m4aSK^-) (24) was subcloned into the pcDNA3 mammalian expression vector (Invitrogen, San Diego, CA) at the *Bam*HI and *Eco*RI sites. For the construction of c-Myc-tagged mGluR4a, the mGluR4a-pcDNA3 plasmid was cut with *Xho*I, and the larger fragment containing pcDNA3 backbone was ligated to itself (the 5′-mGluR4a-pcDNA3 plasmid). The primers *Bst*EII-c-Myc (5′-GT CAC GAA CAA AAG CTT ATT TCT GAA GAA GAC TTG GAT CCA G) and rev-*Bst*EII-c-Myc (5′-GTG ACC TGG ATC CAA GTC TTC TTC AGA AAT AAG CTT TTG TTC) were phosphorylated, annealed to each other, and cloned into the 5′-mGluR4a-pcDNA3 plasmid at the dephosphorylated *Bst*EII site to produce 5′-mGluR4a-c-Myc-pcDNA3. The 931-base pair *Nde*I-*Xho*I fragment from 5′-mGluR4a-c-Myc-pcDNA3 and a 3335-base pair *Xho*I-*Not*I fragment of mGluR4a-pcDNA3 were subcloned into pcDNA3 at *Nde*I-*Not*I sites using a three-piece ligation. The c-Myc-tagged mutants were also constructed in this manner using the corresponding mutants.

For the generation of the S157A, S160A, and S181A mutants, the sequences flanking the point of mutation were amplified in two separate PCRs on the rat mGluR4a-pcDNA3 expression plasmid. For all other mutants, the mGluR4a cDNA in pBluescript SK^- (Stratagene) was used as the template. One of four primers used in the generation of each mutant contained the desired mutation. An adjacent primer was phosphorylated prior to PCR, and the two PCR products were ligated to each other and reamplified using the two most distant primers (the 5′-primer from the first PCR and the 3′-primer from the second PCR). The resulting products were cut with the appropriate restriction enzymes and subcloned in place of the corresponding wild-type fragment. All expression constructs were assembled in the pcDNA3 mammalian expression vector for transient transfection in HEK cells. In all cases, the orientation of the inserts and the integrity of subcloning sites were checked by restriction analysis where applicable, and the PCR-amplified regions were sequenced to confirm the mutations and to ensure that no other changes were introduced.

A cassette mutagenesis method was used to construct the S159A mutation. A 1.79-kilobase *Kpn*I fragment of mGluR4a containing Ser^{159} was subcloned into the pBluescript SK^- vector and transformed into CJ236 bacteria. A mutagenic oligonucleotide (5′-GGA GCT TCA GGG GCC TCC GTC TCG ATC A-3′) was annealed to the template and used to make double-stranded mutant DNA with T4 DNA polymerase and T4 ligase. The double-stranded mutant DNA was transformed into DH5α cells (Life Technologies, Inc.), and rapid screening of the colonies was carried out using the *Sac*I restriction enzyme; the DNA from a positive colony was sequenced to confirm the presence of the S159A mutation and the absence of any additional base pair changes. The mutated cassette was then excised from pBluescript SK^- and ligated back in the correct orientation in the mGluR4a cDNA in pcDNA3.

HEK cells were cultured in modified Eagle's medium with 6% fetal bovine serum and antibiotics. Transient transfections were conducted using the protocol described previously (22); all experiments were conducted on cells or membranes collected 48 h after transfection.

Radioligand Binding Assay—The membrane preparation procedure and the L-[^{3}H]AP4 binding assay were carried out as described by Eriksen and Thomsen (25), except that 300 μM L-SOP was used to define nonspecific binding. Bound and free radioligands were separated by centrifugation. For competition experiments, 30 nM L-[^{3}H]AP4 was used. The data were analyzed using GraphPAD Prism software. L-[^{3}H]AP4 (specific activity, 54 Ci/mmol), L-SOP, sodium L-glutamate, (2*S*,3*S*,4*S*)-CCG/(2*S*,1′*S*,2′*S*)-2-(carboxycyclopropyl)glycine (L-CCG-1), and (*RS*)-α-cyclopropyl-4-phosphonophenylglycine (CPPG) were purchased from Tocris (Bristol, United Kingdom)

Immunoblotting and Immunocytochemistry—The procedures for immunoblotting were carried out as described by Pickering *et al.* (26). Electrophoresis samples containing 100 mM dithiothreitol were incubated at 37 °C for 15 min prior to gel electrophoresis. Antibodies raised in rabbits against the carboxyl terminus of mGluR4a were generated as described by Risso Bradley *et al.* (4) and Petralia *et al.* (27). For immunocytochemical analyses, HEK cells were washed with phosphate-buffered saline (PBS) for 2 × 2 min at 48 h post-transfection and fixed with PBS containing 4% paraformaldehyde and 4% sucrose for 10 min at 25 °C. The cells were air-dried for 15 min and then incubated in 10% bovine serum albumin in PBS for 30 min at 25 °C. The cells were subsequently incubated for 1 h at 25 °C with either the anti-mGluR4a antibody or with anti-c-Myc mouse monoclonal IgG_1 (Upstate Biotechnology, Inc.) diluted to a final concentration of 0.15 μg/ml in 3% bovine serum albumin in PBS. The primary antibody was then removed, and the cells were washed 5 × 5 min with PBS. After washing, the cells were incubated for 60 min at 25 °C with biotin-conjugated anti-mouse IgG (Sigma, B 0529) diluted to a final concentration of 2.75 μg/ml in 3% bovine serum albumin in PBS. After incubation, the cells were washed 5 × 5 min with PBS and treated with fluorescein isothiocyanate-conjugated ExtrAvidin (Sigma, E 2761) diluted to a final concentration of 5 μg/ml in 3% bovine serum albumin in PBS for 60 min at 25 °C in the dark; the cells were washed 4 × 5 min with PBS, mounted with 50% glycerol solution in PBS, and photographed with a Zeiss Axiovert 135 TV microscope equipped with a 485-nm excitation and 530-nm emission filter at a magnification of ×400.

Measurements of Intracellular Calcium—HEK cells were subcultured onto six-wells plates 1 day before transfection at 50% confluency. The cells were cotransfected with 4 μg of mGluR4a cDNA or mutant cDNAs and 4 μg of G_{qi9} cDNA in the pcDNA1 vector (28). At 24 h post-transfection, the cells were plated onto 35-mm dishes (Nunc) fitted with glass coverslips (Bellco Glass, Inc.) previously coated overnight at 37 °C with poly-L-ornithine (0.01%, M_r 40,000; Sigma) to increase adhesion of the cells. At 48 h post-transfection, the cells were washed 3 × 5 min at 37 °C in wash buffer (135 mM NaCl, 5.4 mM KCl, 1.8 mM $CaCl_2$, 0.9 mM $MgCl_2$, and 10 mM HEPES, pH 7.4), and then loaded for 45 min at 37 °C with 6 μM fura-2 acetoxymethyl ester (Molecular Probes, Inc.) dissolved in wash buffer. After loading, the cells were washed 3 × 10 min with wash buffer prior to recording. Fluorescence recordings were made on single cells using a dual excitation imaging system (Universal Imaging Corp.) equipped with a Zeiss Axiovert 135 microscope.

RESULTS

Molecular Modeling—The ATD of mGluR4 extends from the amino terminus to the first putative transmembrane domain and encompasses the initial 66 kDa of the receptor protein (Fig. 1). The molecular model of the ATD of mGluR4 retains the salient characteristics of the bacterial periplasmic binding proteins. These include two domains of similar shape connected by a hinge region made up of three interdomain crossover seg-

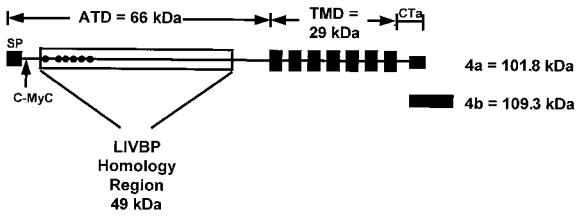

FIG. 1. **Schematic representation of the major domains of the mGluR4 protein.** The two splice variants of mGluR4 (mGluR4a and mGluR4b) (30) that differ only in their carboxyl-terminal sequences are indicated. The position of the segment of the ATD of mGluR4 that is homologous to LIVBP is indicated by the *open box*; the *black circles* within this box denote the relative positions of the point mutations examined (R78A, S157A, S159A, S160A, S181A, and T182A). *CTa*, carboxyl-terminal domain of mGluR4a; *TMD*, transmembrane domains (indicated by the *seven black boxes*); *SP*, signal peptide. *C-MyC* indicates the point of insertion of the 12-amino acid c-Myc epitope tag.

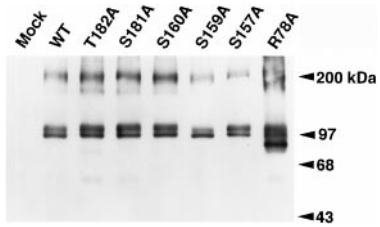

FIG. 2. **Immunoblot of mock-transfected, wild-type, and mutant mGluR4 receptors expressed in HEK cells.** Each lane contained 10 μg of protein; the blot was labeled with the antibody to the carboxyl terminus of mGluR4a. *WT*, wild-type mGluR4.

ments (11, 29). The large insertions at amino acids 1–46, 125–149, 353–401, and 426–439 that were not included in the model are all well separated from the proposed ligand-binding site located in a cavity formed between the two domains. This site is analogous to the leucine-binding site found in LIVBP. In this cavity, the agonist L-SOP is held in place by hydrogen bond interactions with both main chain and side chain atoms and complementary ionic interactions with charged residues. With the exception of hydrogen bonds between the ligand and the peptide backbone of the binding domain, these interactions can be disrupted by substituting the natural amino acids with alanine. Thus, a series of mutations were made at selected residues that were anticipated to interact directly with the ligand (Arg^{78}, Ser^{159}, and Thr^{182}) and at amino acids that may be indirectly involved in binding (Ser^{157} and Ser^{181}). The model predicted that Ser^{160} lies outside of the binding pocket, and therefore mutation of this residue to alanine was not likely to affect ligand binding.

Expression of Mutant Proteins—To determine whether any of the point mutations affected protein expression, immunoblots of cells transiently transfected with mGluR4a or with the R78A, S157A, S159A, S160A, S181A, or T182A mutant were probed with an antibody raised against the carboxyl terminus of mGluR4a. Labeled bands with relative molecular masses of ~96 and 100 kDa, which likely correspond to the non-glycosylated and glycosylated forms of mGluR4, respectively, were observed in samples of wild-type and c-Myc-tagged mGluR4a and in all of the mutants (Fig. 2). Higher molecular mass dimers of mGluR4 were also present as previously reported in mouse cerebellum (7). The R78A mutant also showed an additional immunoreactive band at ~90 kDa; the nature of this band is not known. Nevertheless, the intensity of the monomer bands at 96 and 100 kDa was similar to that of the wild-type receptor in all mutants including R78A, demonstrating that none of the point mutations produced any substantial alterations in the level of protein expression. The similarity in the expression levels of wild-type mGluR4a and the S157A, S160A, and S181A mutants was also indicated by the similar B_{max} values in the radioligand binding experiments (see below).

Pharmacological Analyses of Epitope-tagged and Mutant Receptors—Saturation analyses of L-[^{3}H]AP4 binding to membranes prepared from HEK cells transfected with the wild-type mGluR4a expression plasmid showed a dissociation constant (K_D) and maximum number of binding sites (B_{max}) of 504 nM and 8.6 pmol/mg, respectively (Fig. 3*A* and Table I). The dissociation constant for mGluR4a expressed in HEK cells was similar to that reported previously for mGluR4a expressed in hamster kidney cells (K_D = 441 nM) (25) and in insect Sf9 cells (K_D = 480 nM) (30). A modified expression vector was also constructed in which a c-Myc epitope tag was inserted immediately downstream of the proposed signal peptide (Fig. 1). The insertion of the c-Myc tag at this position was done (*a*) to provide an extracellular antibody epitope to facilitate immunocytochemical labeling (see below) and (*b*) to ensure that the tag would not be cleaved by signal peptidases. c-Myc-tagged mGluR4a displayed K_D and B_{max} values of 404 nM and 8.7 pmol/mg, respectively (Fig. 3*B* and Table I); neither value was significantly different ($p > 0.05$, one-way analysis of variance and Dunnett's multiple comparison test) from that of the untagged receptor, indicating that the insertion of the epitope at this site did not affect ligand affinity or the level of expression of mGluR4a.

The molecular model of the ATD of mGluR4 suggests that Arg^{78}, Ser^{159}, and Thr^{182} interact directly with the glutamate ligand. When mutated to alanine, all three residues produced receptors that were nearly devoid of the ability to bind L-[^{3}H]AP4 (Fig. 4). The R78A, S159A, and T182A mutants displayed 2 ± 0.8, 5 ± 1, and 4 ± 2% (mean ± S.E. of three experiments) of control (wild-type mGluR4a) binding, respectively. Due to the very low level of binding of the radioligand, it was not possible to obtain estimates of affinities for these two mutants in saturation or competition experiments. To further probe the ligand-binding domain of mGluR4, several additional mutations were made at amino acid residues that were predicted to be in or very near the binding pocket, but not directly involved in ligand binding. Saturation experiments showed that neither the dissociation constants nor the maximum numbers of binding sites of the S157A, S160A, and S181A mutants were significantly different from those of the wild-type receptor ($p > 0.05$, one-way analysis of variance and Dunnett's multiple comparison test) (Table I).

To assess the pharmacological profile of these mutants, competition experiments were conducted using the agonists L-glutamate, L-SOP, and L-CCG-1 and the group III antagonist CPPG (31). The rank order of potency in the S157A, S160A, and S181A mutants was similar to that observed in the wild-type receptor (L-SOP > L-CCG-1 > L-glutamate > CPPG) (Fig. 5). The inhibition constants for these drugs with the S157A and S160A mutants were also similar to those seen with the wild-type receptor (Table II). However, the inhibition constants for the S181A mutant were ~3–5 times higher than those for the wild-type receptor, indicating that this mutation produced a moderate decrease in affinity for the series of compounds tested.

Immunocytochemical Analysis—Although the results from the immunoblot experiments indicated that the R78A, S159A, and T182 mutant polypeptides were translated and expressed at levels comparable to those of the wild-type receptor, it is possible that the very low level of ligand binding of the mutants was caused by misfolding and/or lack of cell-surface expression. To investigate this possibility, an immunocytochemical analysis was carried out on the c-Myc-tagged wild-type receptor, the R78A and T182A mutant receptors, and the untagged S159A

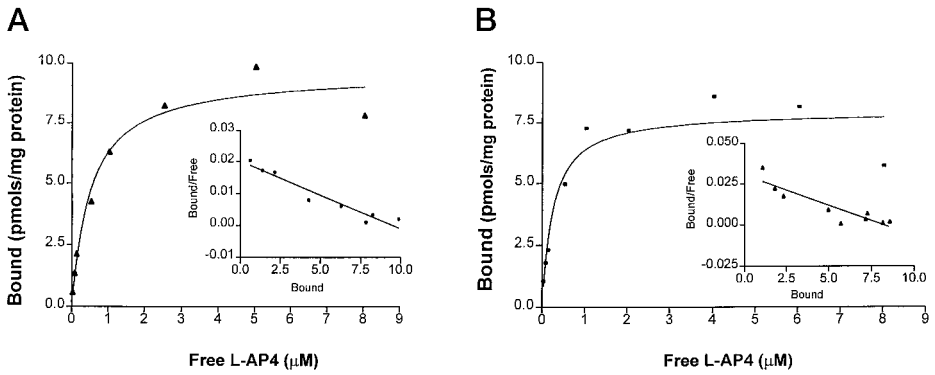

FIG. 3. **Saturation analysis of L-[^{3}H]AP4 binding.** Membranes from HEK cells expressing mGluR4a (*A*) or c-Myc-tagged mGluR4a (*B*) were analyzed in the membrane binding assay. Each experiment was repeated three to four times. *Insets*, Scatchard plots of the saturation data. The K_D and B_{max} values are summarized in Table I.

TABLE I

Affinity constants and maximal binding capacities from L-[^{3}H]AP4 saturation binding analyses conducted on wild-type mGluR4a, c-Myc-tagged mGluR4a, and mutant receptors

Each value is the mean ± S.E. of three to four experiments conducted in triplicate.

mGluR4a	K_D	B_{max}
	nM	*pmol/mg*
WT[a]	504 ± 99	8.6 ± 2.9
c-Myc-WT	404 ± 64	8.7 ± 1.3
S157A	683 ± 52	6.3 ± 1.0
S160A	470 ± 72	5.0 ± 1.6
S181A	570 ± 52	4.2 ± 1.2

[a] Wild-type.

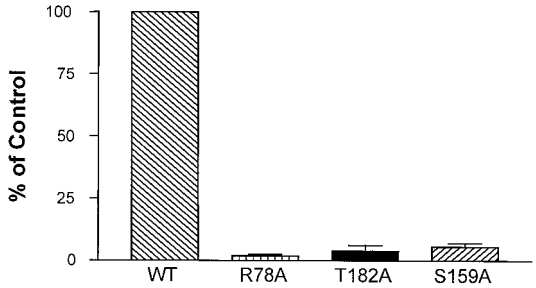

FIG. 4. **Comparison of L-[^{3}H]AP4 binding to membranes prepared from HEK cells expressing wild-type mGluR4a and the R78A, S159A, and T182A mGluR4a mutants.** L-[^{3}H]AP4 binding was conducted at 30 nM L-[^{3}H]AP4. Each *bar* represents the mean ± S.E. of five experiments. *WT*, wild-type mGluR4a.

receptor. Cell-surface expression was assessed by labeling lightly fixed HEK cells (4% paraformaldehyde for 10 min) with the anti-mGluR4a or anti-c-Myc antibody, followed by a biotinylated anti-rabbit or anti-mouse secondary antibody and a fluorescein isothiocyanate-avidin conjugate.

Cells expressing c-Myc-tagged wild-type mGluR4a labeled with the anti-mGluR4a antibody and treated with Triton X-100 to permeabilize the cells showed intense labeling in and particularly around the periphery of the cells, whereas similarly transfected cells not treated with Triton X-100 displayed only background labeling (Fig. 6, *A* and *B*). The absence of specific immunostaining in unpermeabilized transfected cells indicates that the fixation protocol used (without Triton X-100 treatment) did not cause permeabilization of the cells. The immunolabeling pattern observed with the c-Myc-tagged wild-type receptor in unpermeabilized cells labeled with the anti-c-Myc antibody (recognizing the c-Myc epitope in the ATD of mGluR4a; see Fig. 1) was similar to the pattern seen with the anti-mGluR4a antibody in permeabilized cells (data not shown). In unpermeabilized cells expressing the c-Myc-tagged R78A mutant receptor and labeled with the anti-c-Myc antibody (Fig. 6*C*) and in Triton X-100-permeabilized cells labeled with the anti-mGluR4a antibody (Fig. 6*D*), the pattern and intensity of cell-surface labeling were similar to those seen with the wild-type receptor. Cell-surface expression of the S159A (Fig. 6*E*) and T182A (Fig. 6*F*) mutants was also essentially identical to that observed with wild-type mGluR4a. Together, the results of these experiments demonstrate that the cell-surface expression of the R78A, S159A, and T182A mutants was similar to that of wild-type mGluR4a.

Functional Analysis of Mutant Receptors—To establish that the wild-type receptor and the S157A, S160A, and S181A mutants expressed in HEK cells were functional receptors and to generate EC_{50} values, attempts were made to measure the inhibition of cAMP formation after stimulation by forskolin. However, despite receptor expression and a robust forskolin-induced increase in cAMP, the effects of glutamate and other agonists were too weak to accurately estimate EC_{50} values in this system. As an alternative qualitative assessment of receptor activity, the activation of the receptors by L-glutamate was monitored by measuring increases in intracellular calcium in cells cotransfected with cDNAs coding for mGluRs and the chimeric G-protein G_{qi9} (28). Gomeza *et al.* (2) have shown that G_i-linked mGluRs can couple to this modified G-protein and activate phospholipase C. In the present experiments, the activation of inositol 1,4,5-triphosphate-sensitive calcium stores in cotransfected HEK cells was analyzed by measuring the fluorescence induced by the binding of intracellular calcium to fura-2. Although the magnitude of the calcium levels varied somewhat from cell to cell and transfection to transfection, this technique can be used to demonstrate functional coupling of G_i-linked receptors. Most cells expressing the wild-type receptor or the mutants cotransfected with G_{qi9} displayed glutamate-induced increases in intracellular calcium, whereas mock-transfected cells or cells transfected with only the mGluR4a cDNA did not respond to glutamate (Fig. 7). In two separate experiments (transfections), the ratios of cells showing a response out of the total number of cells analyzed were as follows: mock-transfected, 0:12; mGluR4a only, 0:25; mGluR4a + G_{qi9}, 34:50; S157A + G_{qi9}, 17:24; S160A, 18:24; and S181A, 28:36.

DISCUSSION

The amino-terminal portions of the ATDs of mGluRs are homologous to prokaryotic LIVBP, whereas two discontinuous segments of the ionotropic glutamate receptors are homologous to the bacterial lysine/arginine/ornithine-binding protein (11, 32, 33). Our model of the ATD of mGluR4 maintains the general structural characteristics of the bacterial periplasmic binding proteins. It consists of two lobes connected by a hinge region, which, in the open configuration, forms a cleft where the ligand can enter. After ligand binding, the cleft closes to form a binding pocket, where the ligand is sequestered from the surrounding solvent (Fig. 8). The amino acids mutated in this study were all located within a region of the ATD of mGluR4 that forms part of the amino-terminal segment of the bilobed

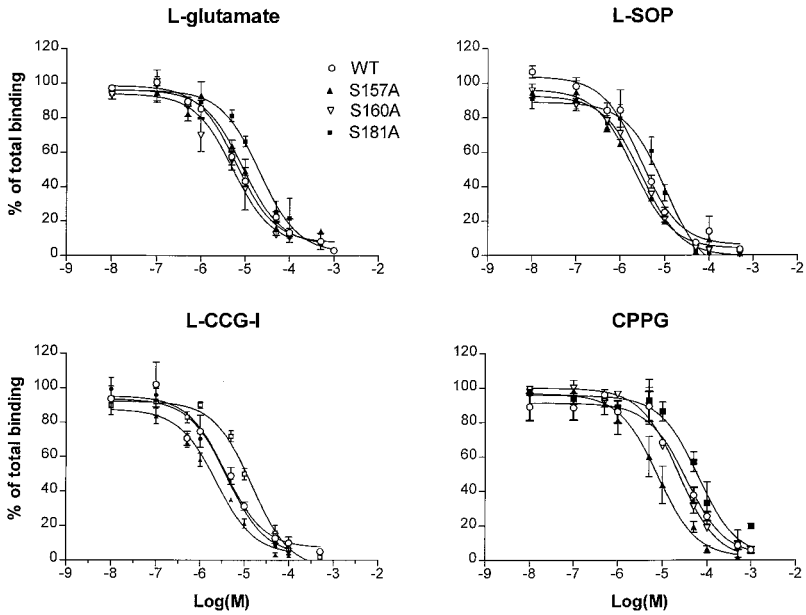

FIG. 5. **Radioligand binding competition experiments with wild-type mGluR4a and the S157A, S160A, and S181A mutants.** All experiments were carried out using 30 nM L-[^{3}H]AP4. Each *point* represents the average of three experiments; *error bars* depict S.E. The inhibition constants are listed in Table II. *WT*, wild-type mGluR4a.

TABLE II

Inhibition constants of various drugs for L-[^{3}H]AP4 binding to wild-type mGluR4a and the S157A, S160A, and S181A mutants

The concentration of L-[^{3}H]AP4 was 30 nM. Data are the means ± S.E. of three experiments.

mGluR4a	IC_{50}			
	L-SOP	L-CCG-1	L-Glutamate	CPPG
			μM	
Wild-type	2.7 ± 0.5	4.0 ± 1.5	5.7 ± 0.5	24 ± 2.7
S157A	2.2 ± 0.5	2.3 ± 0.6	11 ± 3.6	10.3 ± 4.3
S160A	3.2 ± 0.5	3.8 ± 0.3	4.0 ± 2.6	21.3 ± 1.1
S181A	10 ± 2	16 ± 4.1	29 ± 5.3	69 ± 13

"clamshell" part of the ATD. The rationale for targeting selected amino acids for mutagenesis was guided by the model of the ATD of mGluR4, which is, in turn, based on the known three-dimensional structure of LIVBP determined by x-ray diffraction studies (29).

Based on the sequence homology and structural data from crystallographic studies on the bacterial amino acid-binding proteins, O'Hara *et al.* (11) formulated and tested a molecular model of the ATD of the group I receptor, mGluR1. Mutation of either Ser^{165} or Thr^{188} in the ATD of mGluR1 caused substantial reductions in the agonist-evoked stimulation of phosphatidylinositol hydrolysis and in the binding of L-[^{3}H]glutamate, suggesting that these amino acids may be involved in ligand recognition. Ser^{165} and Thr^{188} of mGluR1 align with Ser^{159} and Thr^{182} of mGluR4 (see Fig. 9*B* for a compilation of equivalent residues mutated in mGluR1, mGluR4, $GABA_B$ receptors, and LIVBP). Although the amino acid sequence of rat mGluR4 is only 43% identical to that of rat mGluR1 and the two receptors display different pharmacological and biochemical profiles, our results indicate that at least three conserved amino acids in the ATDs of mGluRs may be key determinants of ligand binding to all members of the mGluR family.

In the molecular model of the ATD of mGluR4, mutations at Arg^{78}, Ser^{159}, and Thr^{182} were predicted to have a major impact on L-[^{3}H]AP4 binding, whereas mutations at Ser^{157}, Ser^{160}, and Ser^{181} were predicted to have less dramatic effects on binding; our experimental results have corroborated the predictions of the molecular model of mGluR4. The substantial reductions in L-[^{3}H]AP4 binding in the R78A, S159A, and T182A mutants suggest that these amino acids are directly involved in ligand recognition. It is unlikely that the large decrease in binding was caused by a reduction in protein expression and/or misfolding of the mutant receptors because immunoblot and immunocytochemical analyses demonstrated that both mutants were expressed at similar levels and showed similar cell-surface expression patterns compared with the wild-type receptor.

The drastic reduction in L-[^{3}H]AP4 binding in the S159A mutant agrees with the loss of activity seen in the analogous mutation in mGluR1 (Ser^{165}) (11). Our molecular model suggests that the hydroxyl group on the side chain of this serine forms a hydrogen bond with the α-carboxylic acid group on the glutamate ligand (Fig. 8). The nearly complete loss of L-[^{3}H]AP4 binding in the Arg^{78} mutant indicates that this amino acid is another crucial feature of the ligand recognition motif in mGluR4. Although no equivalent mutation has been made in other mGluRs, this arginine is also conserved in all mGluRs, and it is well positioned for such an interaction. The orientation of the ligand in the binding pocket places the γ-carboxy group on the side chain of L-glutamate in close proximity to the positive charge on the side chain of Arg^{78} (Fig. 8). We postulate that an ion pair between the γ-carboxyl group on the side chain of L-glutamate or the γ-phosphonate group on L-SOP or L-AP4 and the amino group on the side chain of Arg^{78} is an essential component of the ligand-binding pocket of mGluRs. This suggestion is supported by the fact that this arginine is conserved in all members of the mammalian mGluR family, the salmon brain mGluR, and the *Drosophila* mGluR, but not in the bacterial binding proteins such as LIVBP that mediate the transport of amino acids lacking an acidic side chain.

Mutation of Thr^{182} to alanine in mGluR4 produced a 96% decrease in L-[^{3}H]AP4 binding compared with the wild-type receptor. In mGluR1a, conversion of the analogous threonine (Thr^{188}) to alanine virtually eliminated [^{3}H]glutamate binding (11). The threonine at position 182 of mGluR4 is conserved in 18 homologous proteins, including all eight members of the mammalian mGluR family, an mGluR1 homolog from salmon brain, an mGluR from *Drosophila*, the calcium-sensing receptor, the GBR2 $GABA_B$ receptor subunit, LIVBPs and the leucine-binding proteins from *E. coli* and *Salmonella typhimurium*, and an amide-binding protein (AmiC) from *Pseudomonas aeruginosa*. AmiC has been subclassified with LIVBP and the leucine-binding proteins in "cluster 4" of the bacterial periplasmic binding proteins (34). As is the case with other periplasmic binding proteins, AmiC has low sequence identity to LIVBP (17%), but the overall fold of the protein appears to be

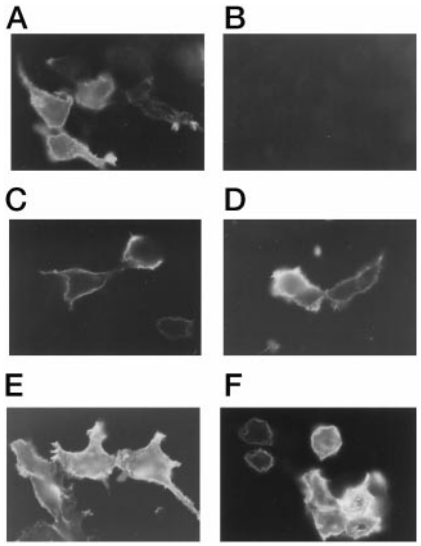

FIG. 6. **Fluorescence immunostaining of transfected HEK cells.** Cells expressing c-Myc-tagged mGluR4a and treated (*A*) or not (*B*) with Triton X-100 to permeabilize the cells were labeled with the anti-mGluR4a antibody. Cells expressing c-Myc-tagged R78A without permeabilization and labeled with the anti-c-Myc antibody (*C*) and c-Myc-tagged R78A-expressing cells permeabilized with Triton X-100 and immunolabeled with the anti-mGluR4a antibody (*D*) showed cell-surface expression similar to that seen with the wild-type receptor. Permeabilized cells expressing the untagged S159A mutant receptor and labeled with the anti-mGluR4a antibody (*E*) and unpermeabilized cells expressing the c-Myc-tagged T182A mutant and labeled with the anti-c-Myc antibody (*F*) also displayed cell-surface expression as observed with the wild-type receptor.

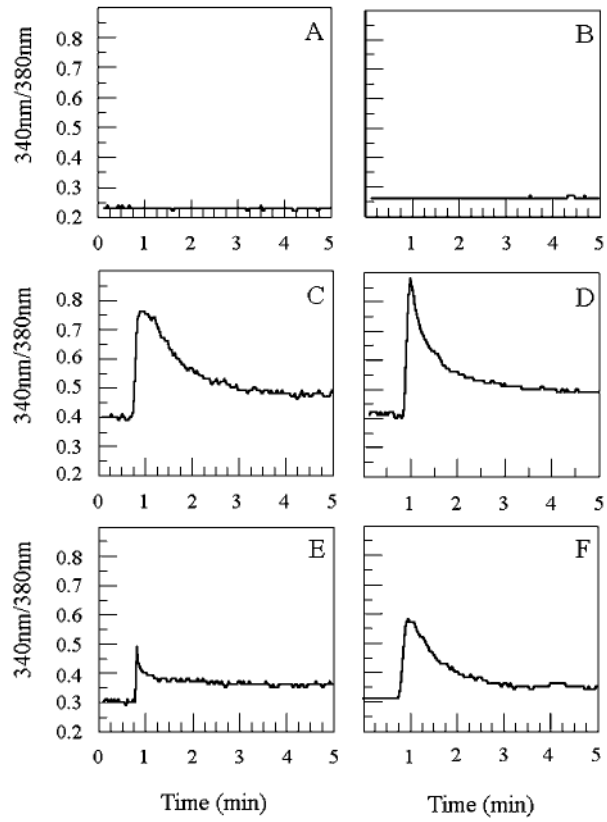

FIG. 7. **Representative recordings of intracellular calcium release from HEK cells cotransfected with mGluRs and G_{qi9}.** *A*, mGluR4a only; *B*, untransfected cells; *C*, mGluR4a + G_{qi9}; *D*, S157A + G_{qi9}; *E*, S160A + G_{qi9}; *F*, S181A + G_{qi9}. The cells were loaded with fura-2 acetoxymethyl ester and washed with recording buffer prior to the addition of glutamate (1 mM final concentration) at 0.5–0.75 min after initiation of recording.

similar to that of LIVBP and other members of this subclass of binding proteins (35). Thus, based on these experimental findings, the molecular model of mGluR4, and the high degree of amino acid conservation in the related proteins noted above, we suggest that ligand binding in mGluRs is stabilized by a hydrogen bond formed between the oxygen of the hydroxyl group on the side chain of Thr^{182} and the α-amino group of the ligand (Fig. 8).

In light of the sequence homology between the mGluRs and the $GABA_B$ receptors and the fact that both classes of receptors are activated by amino acids, it is conceivable that some of the determinants of ligand binding to mGluRs may extend to the $GABA_B$ receptor. A sequence alignment of the mGluRs with the $GABA_B$ receptor subunits shows that Ser^{159} of mGluR4 is conserved in GBR1a/b, whereas Thr^{182} of mGluR4 is conserved in the GBR2 protein; in the GBR1a and GBR1b subunits, there is a serine at this position (Fig. 9).

Galvez *et al.* (37) have examined several sites in the GBR1a protein using site-directed mutagenesis; the amino acids mutated included Ser^{246} and Ser^{269}, which align with Ser^{159} and Thr^{182}, respectively, of mGluR4. Mutation of Ser^{246} completely eliminated antagonist binding to GBR1a. Thus, this serine residue appears to be critical for ligand binding to both mGluRs and $GABA_B$ receptors. Analogous to mGluRs, Ser^{246} of GBR1a/b may form a hydrogen bond with the amino group of GABA. Mutation of Ser^{269} to alanine in GBR1a caused a reduction in affinities for various $GABA_B$ receptor ligands; these changes in affinity ranged from a 5- to 50-fold decrease in affinity depending on the ligand. Based on the relatively modest effects on binding, Galvez *et al.* (37) suggested that Ser^{269} of GBR1a was likely not directly involved in ligand binding to the $GABA_B$ receptor. However, the threonine at the equivalent position of the GBR2 subunit (Fig. 9*A*) has not yet been assessed in mutagenesis studies and this subunit is obligatory for reconstituting wild-type pharmacology (15, 16). Additional mutagenesis experiments on the ligand-binding site of heteromeric $GABA_B$ receptors may help to clarify both the similarities and the unique characteristics of the binding domains within the mGluRs and the $GABA_B$ receptors.

In addition to R78A, S159A, and T182A, several additional mutations were made at amino acids that are positioned within or near the ligand-binding pocket. Ser^{181} may be located in close proximity to Ser^{159}. As noted above, the hydroxyl groups on the side chains of Ser^{159} of mGluR4 and Ser^{165} of mGluR1 may form hydrogen bonds with the α-carboxyl group of the ligand. The position of the hydroxyl group on the side chain of Ser^{181} close to the side chain of Ser^{159} of mGluR4 suggests the possibility that the precise positioning of Ser^{159} might be dependent upon hydrogen bonding between the side chains of the two amino acids. The data from the competition experiments, in which mutation of Ser^{181} to alanine resulted in an ~4-fold increase in the IC_{50} values for the series of drugs tested, support this idea and indicate that Ser^{181} may be indirectly involved in ligand binding through the formation of a hydrogen bond with Ser^{159}.

The model of the ATD indicates that Ser^{160} is situated just outside the binding cavity and is not likely to be involved in ligand recognition, whereas Ser^{157} could be indirectly involved in ligand recognition due to hydrogen bonding to Arg^{78}. In both cases, mutation to alanine produced no discernible effects on L-[^{3}H]AP4 binding. These results indicate that Ser^{160} is likely located outside of the ligand-binding pocket and that if a hydrogen bond between Ser^{157} and Arg^{78} does exist, it is not critical for ligand binding. Ser^{160} of mGluR4 is conserved in all other members of the mGluR family except mGluR2, which has

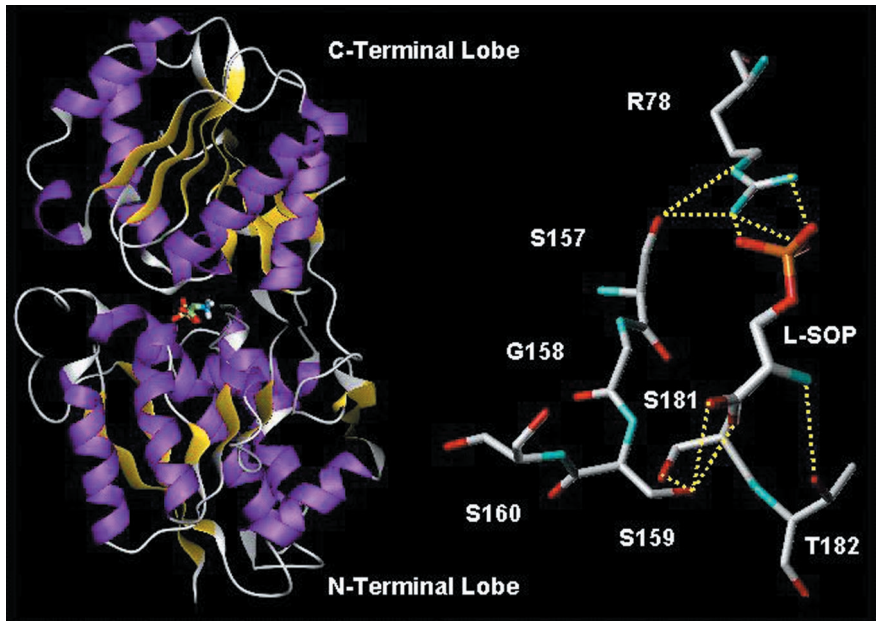

FIG. 8. **Model of the ligand-binding domain of mGluR4 based on the three-dimensional structure of the closed form of LIVBP.** The *left panel* depicts a C-α trace of the ATD illustrating the fold of the polypeptide backbone together with the docked L-SOP ligand; *yellow* depicts β-strands, and *magenta* represents α-helices. Regions of the mGluR4 ATD that were not homologous to LIVBP were not included in the model. The secondary structure of the two lobes consists primarily of β-sheets flanked by α-helices. The *right panel* shows a close-up view of the ligand-binding site in mGluR4 highlighting the proposed interactions between L-SOP and selected residues in the proposed binding pocket. *Orange*, phosphorus; *red*, oxygen; *turquoise*, nitrogen; *white*, carbon. For clarity, the hydrogen atoms are not shown.

A.

```
mGluR4      47   GDITLGGLFPVHGRG----SEGKACGELKKEKGIHRLEAMLFALDRINNDPDLLP-NITL
mGluR1      43   GDVIIGALFSVHHQPPAEKVPERKCGEIREQYGIQRVEAMFHTLDKINADPVLLP-NITL
LIVBP        1   EDIKV-AVVGAMSGP-------------VAQYGDQEFTGAEQAVADINAKGGIKG-NKLQ
GBR2        50   PSSPPLSIMGLMPLT-------K--EVAKGSIGRGVLPAVELAIEQIRNESLLRP-YFLD
GBR1a      164   SERRAVYIGALFPMS------------GGWPGGQACQPAVEMALEDVNSRRDILPDYELK

mGluR4     102   GARILDTCSRDTHALEQSLTFVQ-ALI----EKDGTEVRCGSGG---PPIITKPERVVGV
mGluR1     102   GSEIRDSCWHSSVALEQSIEFIRDSLISIRDEKDGLN-RCLPDGQTLPPGRTKKP-IAGV
LIVBP       46   IAKYDDACDP-----KQAVAVAN---K-------VVN-----DG------------IKYV
GBR2       100   LRLYDTECDN-----AKGLKAFYD--A--------IK-----YG----PN------HLMV
GBR1a      212   LIHHDSKCDP-----GQATKYLY---------ELLYN-----DP------------IKII

mGluR4     154   IGASGSSVSIMVANILRLFKIPQISYASTAPDLSDNSRYDFFSRVVPSDTYQAQ-AMVDI
mGluR1     160   IGPGSSVAIQVQNLLQLFDIPQIAYSATSIDLSDKTLYKYFLRVVPSDTLQAR-AMLDI
LIVBP       74   IGHLCSSSTQPASDIYEDEGILMITPAATAPELTARG-YQLILRTTGLDSDQGPTAAKYI
GBR2       130   FGGVCPSVTSIIAESLQGWNLVQLSFAATTPVLADKKKYPYFFRTVPSDNAVNP-AILKL
GBR1a      241   LMPGCSSVSTLVAEAARMWNLIVLSYGSSSPALSNRQRFPTFFRTHPSATLHNP-TRVKL
```

B.

mGluR4	R78	S159	T182
mGluR1	R77	S165	T188
LIVBP	E22	S79	T102
GBR1a	C187	S246	S269

FIG. 9. **Multiple sequence alignment of mGluR1, mGluR4, LIVBP from *E. coli*, and the $GABA_{B1a}$ and $GABA_{B2}$ receptor subunits.** In *A*, portions of the ATDs of the rat receptor proteins that are homologous to LIVBP are shown. The sequences were aligned using Clustal W (Version 1.74). *Boldface* residues indicate Arg^{78}, Ser^{159}, and Thr^{182} of mGluR4 and the homologous amino acids in the related proteins. The segment of the amino acid sequence shown for the GBR1a protein is identical to this region in the GBR1b splice variant. In *B*, conversion table is shown for amino acid numbering based on multiple sequence alignment of equivalent amino acids in the binding pocket of mGluR4, LIVBP, and the rat $GABA_B$ receptor proteins.

an aspartate in this position. Interestingly, Kubo *et al.* (36) have reported that mGluR1, mGluR3, and mGluR5 are activated by millimolar concentrations of extracellular calcium in the absence of L-glutamate and that the serine residues at this position (equivalent to Ser^{160} of mGluR4) in wild-type mGluR1, mGluR3, and mGluR5 are required for activation by calcium. Mutation of the aspartate in mGluR2 to serine confers calcium sensitivity to mGluR2, whereas conversion of the analogous serines in mGluR1, mGluR3, and mGluR5 to aspartates reduces calcium sensitivity. Consistent with our observation that the S160A mutation in mGluR4 did not affect ligand binding, the mutations affecting calcium activation in mGluR1, mGluR3, and mGluR5 did not affect the EC_{50} values for glutamate activation of mGluR1, mGluR3, and mGluR5 expressed in oocytes (36).

The endogenous ligand for mGluRs is generally assumed to be L-glutamate. However, other amino acids that are present in brain tissue may also act as activators of mGluRs. Although L-AP4 does not exist in the brain, L-SOP is present in micromolar concentrations in the mammalian central nervous system (38). The possibility that substances other than L-glutamate may act as endogenous ligands for mGluRs has been supported by recent findings indicating that the neuropeptide *N*-acetylaspartylglutamate may be a selective ligand for the mGluR3 subtype of mGluR (39). Our data indicating that mGluR4 has an ~2–3-fold higher affinity for L-SOP compared with L-glutamate suggest that L-SOP could act as an endogenous ligand for mGluR4 and other group III mGluRs. The higher affinity of L-SOP for mGluR4 compared with L-glutamate together with the relative selectivity of L-SOP for group III mGluRs suggest that this subclass of mGluRs might be preferentially activated by L-SOP over L-glutamate *in vivo*. Future modeling and mutagenesis studies will likely provide more detailed insight into the molecular basis of the selective activation of group III mGluRs by phosphate-containing amino acids such as L-AP4 and L-SOP.

Acknowledgments—We thank Drs. P. J. Conn, S. Risso Bradley, and R. J. Wenthold for the anti-mGluR4a antibodies; S. Nakanishi and B. R. Conklin for the cDNAs for mGluR4a and G_{qi9}; and J. W. Wells for comments on the manuscript. We also thank Dr. F. A. Quiocho for providing the coordinates for the closed form of the LIVBP.

REFERENCES

1. Pin, J.-P., and Duvoisin, R. (1995) *Neuropharmacology* **34,** 1–26
2. Gomeza, J., Mary, S., Brabet, I., Parmentier, M.-L., Restituito, S., Bockaert, J., and Pin, J.-P. (1996) *Mol. Pharmacol.* **50,** 923–930

3. Macek, T. A., Winder, D. G., Gereau, R. W., IV, Ladd, L. O., and Conn, J. P. (1996) *J. Neurosci.* **76,** 3798–3806
4. Risso Bradley, S., Standaert, D. G., Rhodes, K. J., Rees, H. D., Testa, C. M., Levey, A. I., and Conn, P. J. (1999) *J. Comp. Neurol.* **407,** 33–46
5. Shigemoto, R., Kinoshita, A., Wada, E., Nomura, S., Ohishi, H., Takada, M., Flor, P. J., Neki, A., Abe, T., Nakanishi, S., and Mizuno, N. (1997) *J. Neurosci.* **17,** 7503–7522
6. Stowell, J. N., and Craig, A. M. (1999) *Neuron* **22,** 525–536
7. Pekhletski, R., Gerlai, R., Overstreet, L., Huang, X.-P., Agoypan, N., Slater, N. T., Roder, J. C., and Hampson, D. R. (1996) *J. Neurosci.* **16,** 6364–6373
8. Gerlai, R., Roder, J. C., and Hampson, D. R. (1998) *Behav. Neurosci.* **112,** 1–8
9. Nicoletti, F., Bruno, V., Copani, A., Casabona, G., and Knopfel, T. (1996) *Trends Neurosci.* **19,** 267–272
10. Thomsen, C., and Dalby, N. O. (1998) *Neuropharmacology* **37,** 1465–1473
11. O'Hara, P. J., Sheppard, P., Thøgersen, H., Venezia, D., Haldeman, B. A., McGrane, V., Houamed, K. M., Thomsen, C., Gilbert, T. L., and Mulvihill, E. R. (1993) *Neuron* **11,** 41–52
12. Brown, E. M., Gamba, G., Riccardi, D., Lombardi, M., Butters, R., Kifor, O., Sun, A., Hediger, M., Lytton, J., and Hebert, S. C. (1993) *Nature* **366,** 575–580
13. Ruat, M., Molliver, M. E., Snowman, A. M., and Snyder, S. H. (1995) *Proc. Natl. Acad. Sci. U. S. A.* **92,** 3161–3165
14. Kaupmann, K., Huggel, K., Heid, J., Flor, P. J., Bischoff, S., Mickel, S. J., McMaster, G., Angst, C., Bittiger, H., Froesti, W., and Bettler, B. (1997) *Nature* **386,** 239–246
15. Kuner, R., Kohr, G., Grunewald, S., Eisenhardt, G., Bach A., and Kornau, H.-C. (1999) *Science* **283,** 74–77
16. Ng, G. Y. K., Clark, J., Coulombe, N., Ethier, N., Hebert, T. E., Sullivan, R., Kargman, S., Chateauneuf, A., Tsukamoto, N., McDonald, T., Whiting, P., Mezey, E., Johnson, M. P., Liu, Q., Kolakowski, L. F., Jr., Evans, J. F., Bonner, T. I., and O'Neill, G. P. (1999) *J. Biol. Chem.* **274,** 7607–7610
17. Matsunami, H., and Buck, L. B. (1997) *Cell* **90,** 775–788
18. Moon, M. A., Alder, E., Lindemeier, J., Battey, J. F., Ryba, N. J. P., and Zucker, C. S. (1999) *Cell* **96,** 541–551
19. Tones, M. A., Bendali, H., Flor, P. J., Knopfel, T., and Kuhn, R. (1995) *Neuroreport* **7,** 117–120
20. Takahashi, K., Tsuchida, K., Tanabe, Y., Masu, M., and Nakanishi, S. (1993) *J. Biol. Chem.* **268,** 19341–19345
21. Okamoto, T., Sekiyama, N., Otsu, M., Shimada, Y., Sato, A., Nakanishi, S., and Jingami, H. (1998) *J. Biol. Chem.* **273,** 13089–13096
22. Han, G., and Hampson, D. R. (1999) *J. Biol. Chem.* **274,** 10008–10013
23. Blundell, T. L., Sibanda, B. L., Sternberg, M. J. E., and Thornton, J. M. (1987) *Nature* **326,** 347–352
24. Tanabe, Y., Masu, M., Ishii, T., Shigemoto, R., and Nakanishi, S. (1992) *Neuron* **8,** 169–179
25. Eriksen, L., and Thomsen, C. (1995) *Br. J. Pharmacol.* **116,** 3279–3287
26. Pickering, D. S., Taverna, F. A., Salter, M. W., and Hampson, D. R. (1995) *Proc. Natl. Acad. Sci. U. S. A.* **92,** 12090–12094
27. Petralia, R. S., Wang, Y.-X., Niedzielski, A. S., and Wenthold, R. J. (1996) *Neuroscience* **71,** 949–976
28. Conklin, B. R., Farfel, Z,, Lustig, K. D., Julius, D., and Bourne, H. R. (1993) *Nature* **363,** 274–276
29. Sack, J. S., Saper, M. A., and Quiocho, F. A. (1989) *J. Mol. Biol.* **206,** 171–191
30. Thomsen, C., Pekhletski, R., Haldeman, B., Gilbert, T. A., O'Hara, P. J., and Hampson, D. R. (1997) *Neuropharmacology* **36,** 21–30
31. Toms, N. J., Jane, D. E., Kemp, M. C., Bedingfield, J. S., and Roberts, P. J. (1996) *Br. J. Pharmacol.* **119,** 851–854
32. Sutcliffe, M. J., Wo, Z. G., and Oswald, R. E. (1996) *Biophys. J.* **70,** 1575–1589
33. Sutcliffe, M. J., Smeeton, A. H., Wo, Z. G., and Oswald, R. E. (1998) *Methods Enzymol.* **293,** 589–619
34. Tam, R., and Saier, M. H., Jr. (1993) *Microbiol. Rev.* **57,** 320–346
35. Chamberlain, D., O'Hara, B. P., Wilson, S. A., Pearl, L. H., and Perkins, S. J. (1997) *Biochemistry* **36,** 8020–8029
36. Kubo, Y., Miyashita, T., and Murata, Y. (1998) *Science* **279,** 1722–1725
37. Galvez, T., Parmentier, M.-L., Joly, C., Malitschek, B., Kaupmann, K., Kuhn, R., Bittiger, H., Froestl, W., Bettler, B., and Pin, J.-P. (1999) *J. Biol. Chem.* **274,** 13362–13369
38. Klunk, W. E., McClure, R. J., and Pettegrew, J. W. (1991) *Mol. Chem. Neuropathol.* **15,** 51–72
39. Wroblewska, B., Wroblewski, J. T., Pschenichkin, S., Surin, A., Sullivan, S. E., and Neale, J. H. (1997) *J. Neurochem.* **69,** 174–181